Food and Chemical Toxicology 125 (2019) 383–391

Contents lists available at ScienceDirect

Food and Chemical Toxicology

journal homepage: www.elsevier.com/locate/foodchemtox

Inhibitory effects of compounds isolated from *Lepechinia meyenii* on tyrosinase

María Inés Crespo[a], Macarena Funes Chabán[a], Priscila Ailín Lanza[b], Mariana Belén Joray[a], Sara María Palacios[a], D. Mariano Adolfo Vera[b,**], María Cecilia Carpinella[a,*]

[a] Fine Chemical and Natural Products Laboratory, School of Chemistry, IRNASUS-CONICET, Catholic University of Córdoba, Avda. Armada Argentina 3555, X5016DHK, Córdoba, Argentina
[b] Department of Chemistry, QUIAMM – INBIOTEC –CONICET, College of Exact and Natural Sciences, National University of Mar del Plata, Mar del Plata, Argentina

ARTICLE INFO

Keywords:
Phenolic acids
Tyrosinase inhibitors
Molecular docking
Lepechinia meyenii

ABSTRACT

To contribute enzymatic browning inhibitors to the food industry and also extend knowledge about the phytochemical profile of the anti-tyrosinase plant *Lepechinia meyenii*, its ethanol extract was subjected to bioguided fractionation. Three hydroxycinnamic acids, *p*-coumaric acid (**1**), caffeic acid (**2**) and rosmarinic acid (**3**), were isolated as mainly responsible for its activity. Compounds **1**, **2** and **3** showed themselves highly effective for inhibiting tyrosinase with IC_{50} values of 0.30, 1.50 and 4.14 μM, respectively, for monophenolase activity and 0.62, 2.30 and 8.59 μM, respectively for diphenolase activity. This is the first report describing the isolation of the compounds causing the tyrosinase inhibitory activity of *L. meyenii* extract. The inhibitory kinetics of **1–3** using both L-tyrosine and L-DOPA as substrates was investigated and the results obtained were discussed at molecular level by docking analysis. The resulting compounds **1–3** and a phenolic-enriched fraction of the extract, 2.9-fold more active than the starting material, may be suitable as non-toxic and inexpensive alternatives for the control of deleterious enzymatic darkening.

1. Introduction

Tyrosinase (EC 1.14.18.1, Syn polyphenol oxidase PPO) is a copper-containing oxygenase that plays a critical role in the food industry due to its participation in the enzymatic browning of shellfish and plant-derived foods and beverages. This process takes place when the enzyme and its polyphenolic substrates are mixed during post-harvest processing and storage (Chiari et al., 2010). Although the darkening reaction improves the quality of certain products (He et al., 2008), it is also the main cause of undesirable change in the colour of agricultural products, with losses of up to 50% in vegetables and fruits (Jukanti, 2017). In addition, enzymatic browning reduces the market value of shellfish due to the deleterious appearance of its cuticle (Coates and Nairn, 2013). During the darkening, tyrosinase catalyzes the hydroxylation of monophenols to *o*-diphenols, and the oxidation of these to the corresponding *o*-quinone, which then polymerizes to form the final dark brown pigments (Larik et al., 2017). *o*-Quinones are powerful electrophiles, which can suffer nucleophilic attack by water, other polyphenols, amino acids, peptides and proteins (Rouet-Mayer et al., 1990) leading to a diminished digestibility and nutritional quality of food as well as to the formation of toxic compounds (Friedman, 1996; Kim and Uyama, 2005). Identifying inhibitors of tyrosinase to maintain the appearance, flavour, texture and nutritional value of many horticultural and sea products remains a challenge for academia and industry.

Over the years, plants have attracted interest as a source of compounds with different bioactivities (Carpinella and Rai, 2009; Cespedes et al., 2013; Gonzalez et al., 2017, 2018; Joray et al., 2011, 2015, 2017; Palacios et al., 2010; Rai and Carpinella, 2006) and market studies have confirmed that there is increasing global demand for plant-derived products (Bart and Pilz, 2011). In most cases, inhibitors from natural sources are considered free of harmful side effects and, therefore, to have great potential in the food industry (Kim and Uyama, 2005; Maisuthisakul and Gordon, 2009). Although the literature on tyrosinase inhibitors of plant origin is extensive (Kim and Uyama, 2005; Lee et al., 2016; Wu, 2014), it is estimated that only 6 and 15% of terrestrial flora have been evaluated pharmacologically and phytochemically, respectively, to find bioactive principles (Atanasov et al., 2015). This lack of studies also applies to species of native flora from Argentina, only 1% of

* Corresponding author. Laboratorio de Química Fina y Productos Naturales, Facultad de Ciencias Químicas, Universidad Católica de Córdoba, Avda. Armada Argentina 3555, X5016DHK, Córdoba, Argentina.
** Corresponding author. QUIAMM - INBIOTEC - CONICET, College of Exact and Natural Sciences, National University of Mar del Plata, Mar del Plata, Argentina.
E-mail addresses: dmavera@yahoo.com (D.M.A. Vera), ceciliacarpinella@ucc.edu.ar (M.C. Carpinella).

https://doi.org/10.1016/j.fct.2019.01.019
Received 3 August 2018; Received in revised form 14 January 2019; Accepted 20 January 2019
Available online 23 January 2019
0278-6915/

Abbreviations

DMSO	dimethyl sulfoxide
HPLC-DAD	High-Performance Liquid Chromatography with diode-array detection
L-DOPA	3,4-dihydroxy-L-phenylalanine
MM	molecular mechanical
MTT	3-(4,5-dimethyl-2-thiazolyl)-2,5-diphenyl-2H-tetrazolium bromide
ONIOM	Own N-layered Integrated molecular Orbital and molecular Mechanics
PBMC	peripheral blood mononuclear cells
PHA	lectin from *Phaseolus vulgaris*
QM	quantum mechanical
RMSD	root mean square deviation
TLC	thin layer chromatography
VLC	vacuum liquid chromatography
VMD	visual molecular dynamics

which are considered to have been explored (Gonzalez et al., 2017). The plant kingdom and most Argentinian species thus still constitute an outstanding reservoir of anti-tyrosinase chemical entities.

The great interest in tyrosinase inhibitors encouraged us to search for such chemicals among 91 native plants from central Argentina. This study showed *Dalea elegans, Lepechinia meyenii* and *Lithrea molleoides* to be highly effective in inhibiting phenoloxidase (Chiari et al., 2010). Two highly potent anti-tyrosinase compounds, identified as (Z,Z)-5-(trideca-4,7-dienyl)-resorcinol (Chiari et al., 2010) and 5,2′,4′-trihydroxy-2″,2″-dimethylchromene-(6,7:5″,6″)-flavanone (Chiari et al., 2011) were obtained from *L. molleoides* and *D. elegans*, respectively.

For this study, *L. meyenii*, described for the first time as an anti-tyrosinase plant by our group (Chiari et al., 2010) and lacking information about the metabolites causing this inhibitory effect, was selected as the starting material to identify compounds with promising inhibition on tyrosinase. *L. meyenii* belongs to the Lamiaceae family and is distributed in the west of South America, in the Andes between 1500 and 4500 m, in Argentina, Bolivia and Peru. It is used within the traditional medicinal system of the original peoples of the Peruvian Andes for the treatment of coughs, diarrhoea, burning feeling in the stomach, pain in the joints and as an antispasmodic (de la Cruz et al., 2014; Hammond et al., 1998). The ethanol extract of *L. meyenii* showed antibacterial activity (Rojas et al., 2003). Nevertheless, only two reports describe the isolation of compounds from *L. meyenii* extracts (Bruno et al., 1991; Castillo and Lock, 2005).

We describe here the bioguided fractionation and the study of the metabolites causing the anti-tyrosinase activity of *L. meyenii* and, as a consequence, increase the limited knowledge about the phytochemistry of this plant that is suitable for use in food and nutraceutical applications. The kinetics and the mechanisms of inhibition at molecular level of these compounds are discussed. The chemical characteristics of the anti-tyrosinase principles isolated led us to obtain a phenolic-enriched fraction as a promising product for preventing enzymatic browning.

2. Materials and methods

2.1. Plant material and extractions

Lepechinia meyenii (Walp.) Epling was collected from November to March in the hills of Córdoba Province, Argentina. A voucher specimen (UCCOR 233) has been deposited in the 'Marcelino Sayago' Herbarium of the School of Agricultural Science, Catholic University of Córdoba and was authenticated by the botanist, Gustavo Ruiz. For extraction, crushed air-dried plant material (100 g) was extracted for two days with 700 ml ethanol (96%) using Soxhlet. The yield of extract, obtained after exhaustive solvent removal and expressed as percentage weight of air-dried crushed plant material, was 18.25%.

2.2. Chemicals, equipment and reagents

L-Tyrosine, 3,4-dihydroxy-L-phenylalanine (L-DOPA), lyophilised mushroom tyrosinase, lectin from *Phaseolus vulgaris* (PHA) and caffeic, *p*-coumaric and rosmarinic acids were purchased from Sigma–Aldrich (St. Louis, MO). Kojic acid was obtained from Merck (Darmstadt, Germany). Silica gel (70–230 mesh) and Sephadex LH20, both used for column chromatography, were purchased from Sigma–Aldrich. All solvents were HPLC grade. Analytical and preparative thin layer chromatography (TLC) plates were purchased from Analtech (Newark, DE). Sep-pak Plus C18 cartridges were obtained from Waters (Waters, Ireland). ^{1}H and ^{13}C-NMR spectra were recorded with a Bruker AVANCE II 400 spectrometer (Bruker Corporation, Ettlingen, Germany) operated at 400 MHz for ^{1}H and at 100 MHz for the ^{13}C nucleus. Chemical shifts (parts per million) are relative to internal tetramethylsilane used as a reference (d = 0.00). For quantifying the pure compounds, HPLC-DAD was performed on a Shimadzu LC-10 AS (Shimadzu Corp., Tokyo, Japan), equipped with a Luna C18, 250 × 4.6 mm reversed-phase column, eluting with 25% or 50% methanol in water acidified with perchloric acid (pH 2.2) as a mobile phase and UV detection at 210 nm and 320 nm. ClogP values were calculated using ChemDraw Ultra software - CambridgeSoft, Cambridge, UK.

2.3. Bioguided isolation of the active principles from L. meyenii

For the purification process of the tyrosinase inhibitors, the ethanol extract from *L. meyenii* was submitted to vacuum liquid chromatography (VLC) on silica gel with a hexane/diethyl ether/methanol gradient to finally afford six fractions (F1–F6) grouped according to their TLC profile. F4 and F5 showed more than 90% tyrosinase inhibition at 25 μg/ml using L-tyrosine as a substrate and were therefore subjected to additional separation methods for further purification. F4 was fractionated by VLC using the same solvent mixture at increasing gradient. Five fractions were obtained (F4.1-F4.5) and the active F4.2 (90% inhibition at 25 μg/ml), eluted with hexane/diethyl ether 50:50, was further purified in a Sephadex LH-20 column, eluting with hexane/chloroform/methanol 2:1:1 at a flow rate of 1 ml/min. The fractions obtained were grouped in accordance with TLC analysis to finally yield eighteen fractions (F4.2.1-F4.2.18). F4.2.14 and F4.2.15, showing > 95% inhibition at 12 μg/ml, were of high purity, yielding *p*-coumaric acid (**1**) (Fig. 1) (85% purity, by HPLC) and caffeic acid (**2**) (Fig. 1) (80% purity, by HPLC), respectively. F5 was processed by reversed-phase preparative TLC (methanol/water/perchloric acid 10:10:0.01), and a pure compound was obtained as a yellow powder with 70% tyrosinase inhibition at 12 μg/ml. This compound was then identified as rosmarinic acid (**3**) (Fig. 1) (88% purity, by HPLC).

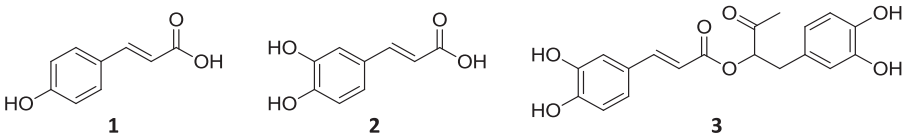

Fig. 1. Chemical structures of *p*-coumaric acid (**1**), caffeic acid (**2**) and rosmarinic acid (**3**).

Isolated compounds were identified by comparison with commercial standards by HPLC-DAD. The ^{1}H and ^{13}C-NMR spectra obtained for these compounds fully matched those previously reported (An et al., 2008; Li et al., 2016; Lin et al., 2011a). Compounds **1–3** were quantified by HPLC and their yields in mg per 100 g of dried and crushed plant material were 6.2; 11.3 and 597.0, respectively, and per 100 g of extract 34, 62 and 32.7 mg, respectively.

2.4. Tyrosinase inhibitory assay

Tyrosinase inhibitory activity was determined according to the method described in our previous reports (Chiari et al., 2010, 2011). Briefly, 2 μl of 2500 U/ml of mushroom tyrosinase was mixed with 10 μl of each fraction or compound to be tested, previously dissolved in ethanol or methanol at the desired concentrations, together with 50 mM phosphate buffer (pH 6.5) to reach a final volume of 160 μl. Ethanol or methanol, or kojic acid, dissolved in 50 mM phosphate buffer, were added as solvent and positive controls, respectively. The reaction mixture was incubated at 37 °C for 90 min with gentle agitation. During this time, the absorbance remained unchanged. Finally, 40 μl of 2.5 mM L-tyrosine or L-DOPA in phosphate buffer were added and the absorbance of each solution was monitored immediately (t = 0) and at 5 or 2 min intervals, respectively, for the formation of dopachrome, which was followed by an increase in absorbance at 450 nm. Measurements were repeated for up to 15 min for monophenolase activity and up to 6 min for diphenolase activity. Differences in absorbance between each time measured and time zero were calculated and the inhibition percentage was determined with respect to the solvent control. The inhibitory effect was calculated as the concentration of inhibitor leading to 50% tyrosinase activity (IC_{50}).

The kinetic behaviour of **1–3** on mushroom tyrosinase was analysed. Experiments were conducted using the same protocol described above with several concentrations of L-tyrosine, L-DOPA or of the inhibitors. The kinetic parameters (Michaelis constant = Km, maximum reaction velocity = Vmax and the inhibitions constants K_I or αK_I) and the type of inhibition were determined by nonlinear regression analysis of the enzyme activity versus the substrate concentration diagram (Graph Pad Prism Software version 7.0, USA), using a Michaelis–Menten kinetic derivation. Lineweaver-Burk plots were created to display the data.

2.5. Preparation of the phenolic fraction from L. meyenii extract

Enrichment in phenolic compounds was performed with a similar method to that described in Chirinos et al. (2008). Briefly, the water-soluble fraction from the ethanol extract was passed through a previously activated C18 Sep-pak cartridge. Polar compounds were eluted with acidified water (0.01% HCl). The resulting phenolic fraction was then eluted with acidified methanol (0.01% HCl). When the methanol was removed, the residue was re-dissolved in water and submitted to a partition with ethyl acetate. The organic phases were assembled and evaporated to dryness. This resulting fraction is referred to as the phenolic fraction and its yield was 20 g per 100 g of extract.

2.6. Determination of the total phenolic content

The total phenolic content of the extract and of the phenolic fraction was measured using the colourimetric Folin-Ciocalteu method (Ainsworth and Gillespie, 2007). Briefly, 100 μl of a properly diluted sample (2 mg/ml in 95% methanol) was added to 8.4 ml of distilled water and mixed with 500 μl of the Folin-Ciocalteu phenol reagent. After 5 min, 1 ml of 15% Na_2CO_3 was added to the solution. The reaction mixture was incubated for 2 h at room temperature, and optical density was measured at 760 nm. A calibration curve was prepared using a standard solution of gallic acid (10 mM, $r^2 = 0.998$). The results were expressed as mol of gallic acid equivalents (GAE) per 100 g of sample.

2.7. Cytotoxicity on peripheral blood mononuclear cells (PBMC)

PMBCs were obtained by density gradient centrifugation (Ficoll) from fresh heparinised blood of healthy human volunteer donors following our reported protocol (Gonzalez et al., 2017, 2018; Joray et al., 2015). The study was approved by the Ethical Committee of the Catholic University of Córdoba Research Ethics Board. Signed informed consents were obtained from donors. For the cytotoxicity assay, 1×10^5 PBMC/well were incubated in duplicate in 96-well plates containing RPMI 1640 with PHA 10 μg/ml, in the presence of increasing concentrations of the extract, the phenolic fraction (0.60–100 μg/ml) or the compounds **1–3** (3–500 μM) or with 1% DMSO (solvent control) for 48 h at 37 °C with 5% CO_2. After incubation, 20 μL of MTT (5 mg/mL) solution was added and the plates were further incubated at 37 °C for 4 h. After removing the incubation medium, the resulting purple formazan crystals were dissolved with 100 μL DMSO. MTT reduction was quantified by determining the absorbance at 595 nm in an iMark micro-plate reader (Bio-Rad, USA) (Gonzalez et al., 2017, 2018; Joray et al., 2015). The percentage of cytotoxicity was determined and the 50% (IC_{50}) inhibition on viability was calculated.

2.8. Molecular modelling

The structural model of the *met* tyrosinase was built from the X-ray structure with the PDB ID 2Y9X of the *Agaricus bisporus* tyrosinase with a tropolone inhibitor co-crystallized (Ismaya et al., 2011). Since this structure corresponds to an inactive form of the enzyme, the right coordination and oxidation states of the current *met* site were rebuilt using a QM/MM protocol. An hydroxide anion was placed between the two copper ions in a similar position to that found in the experimental structure of the *met* form of the apo enzyme (PDB ID 2Y9W). Prior to perform the docking simulations, the charge distribution of the active site was characterised by means of DFT (Density Functional Theory) calculations in a hybrid QM/MM framework. Water molecules, double occupation and other details were fixed and the hydrogens were added using the leap facility of AmberTools (Bayly et al., 1993). The resulting structure were used for a QM/MM energy minimization using the ONIOM (Clemente et al., 2010) implementation of Gaussian 09 (http://www.gaussian.com). The Quantum layer involved the two copper ions, the bridging hydroxide, the six coordinated histidines (H61, H85, H94, H258, H263 and H296) and a cysteine, C83, which is covalently bonded to the imidazole ring of the ligand H85. This layer was treated at the CAM-B3LYP/6-31 + G* level of theory (Yanai et al., 2004) and the rest of the protein was classical with electrostatic embedding using UFF (Rappé et al., 1992) initial charges. The classical portion of the system was held fixed in the positions of the X-ray structure, whilst the quantum part was fully optimized except for the Cα and the backbone H, N, C and O atoms of these quantum amino acids. The charge analysis of the QM atoms was done using MKUFF, with a slight modification of the Merz-Singh-Kollman charges for the ESP and RESP charges with suitable radius for Cu(II) ions (Besler et al., 1990).

These charges fitted the quantum electrostatic potential and thus were further used for the docking simulations. For this last, the Autodock 4.2.6 package (Morris et al., 2009) was used, precomputing a grid inside a box of $36.4 \times 35.4 \times 36.4$ Å^3, roughly centered at the hydroxyl group between the two ions, with a grid spacing of 0.2728 Å. For each inhibitor, 1000 runs of a Lamarckian genetic algorithm (Morris et al., 1998) were performed, each of them with a population of 300 individuals, up to 100,000 generations, with 1 survivor per generation, a limit of 5×10^6 energy evaluation and the remainder algorithm control parameters set to program defaults. The standard Autodock 4.2.6 estimation for the inhibition constants and for the free energy of binding were informed after performing a cluster analysis with a 2.5 Å as criteria for RMSD. The analysis and visualization of results were done using MGLTools and VMD 1.8.7 (Humphrey et al., 1996).

Regarding the *oxy* form of tyrosinase, the same experimental starting structure was used. However, the setup was more complex than for the *met* form, since the coordination site changed remarkably between the two active forms of the enzyme. In first place, the overall electrostatics changed in +1. In addition, and not less relevant, the distance between the Cu(II) ions drastically changed in almost 1 Å, as it could be observed by comparing the 2Y9X to the coordination site of the *oxy* tyrosinase from *Streptomyces castaneoglobisporum* (2ZW9). This change also influenced the position of the coordinating histidines and of the surrounding residues. Finally, and probably the most critical difference, the unusual μ^2-η^2:η^2 bonding involving the couple of Cu(II) ions bridged by a side-on a peroxide ligand, which is expected to draw a different electrostatic potential in the copper ions and in their ligands.

Taking into account all these differences, a very large Quantum region was calculated in the ONIOM protocol and then fully optimized. The quantum layer comprises the same residues as in the *met* form of the enzyme and also including the residues I60, G62, L63, N81, Y82, T84, G86, F90, W93, M280, G281, S282, V283 and P284. The internuclear oxo residue was drawn in the middle of the ions (zoom of the coordination site in Fig. S1; Supplementary material) and allowed to fully optimize, it rendering a set of distances O—O, O—Cu and the corresponding angles very similar to the crystallographic positions of the *oxy* structure 2ZW9 of the bacterium. Residues in contact to them in the classical region were also fully optimized and the rest of the protein heavy atoms were fixed in the crystallographic positions, letting the hydrogens to optimize. From this point, the same full protocol followed for the docking of the *met* tyrosinase was carried out.

2.9. Statistical analysis

All samples were tested at least in triplicate. Statistical analyses were conducted using GraphPad Prism software (Graphpad Prism 7.0, Graphpad Software, Inc., CA, USA). The results are expressed as mean ± SEM. The statistical difference of the inhibitory activity of tyrosinase compared to the positive control or between the extract and the phenolic fraction was calculated by unpaired Student's *t*-test (one-tailed). A p-value < 0.05 was considered as statistically significant. The IC_{50} values were calculated responding to at least five concentrations of each tested sample at a 95% confidence level with upper and lower confidence limits.

3. Results and discussion

3.1. Isolation and structural elucidation of the active compounds from L. meyenii

Responding to the need for new agents with anti-tyrosinase activity and motivated by the limited phytochemical knowledge about the rich flora from Argentina, screening for tyrosinase inhibition was performed with extracts obtained from a large number of native plants (Chiari et al., 2010). This study determined for the first time that the ethanol extract obtained from *L. meyenii* exhibited potent tyrosinase inhibitory activity (Chiari et al., 2010). Based on this promising result, the *L. meyenii* extract was subjected to bioguided fractionation, yielding the hydroxycinnamic acids **1**, **2** and **3** (Fig. 1) as the main agents responsible for its activity. This is the first description of the compounds causing the anti-tyrosinase properties of *L. meyenii*.

3.2. Effects of the isolated compounds on the activity of mushroom tyrosinase

The isolated compounds were subjected to tyrosinase inhibition assay with L-tyrosine or L-DOPA as substrates. The resulting IC_{50} values are summarised in Table 1. The results revealed that compound **1** was the most potent tyrosinase inhibitor, followed by **2** and then **3**.

This result matches that reported by Lee et al., who found that compound **1**, followed by compound **2**, were the most effective for inhibiting tyrosinase among 17 natural compounds assayed (Lee et al., 2012). When L-tyrosine was used as a substrate, **1**, **2** and **3** were respectively 111, 22 or 8 times more active than the positive control, kojic acid ($p < 0.05$) (Table 1), a fungal metabolite that has been used as a food additive to prevent enzymatic browning and as a skin-lightening agent (Burdock et al., 2001). Regarding diphenolase activity, **1**, **2** and **3** were 63, 17 and 4–fold, respectively, more effective tyrosinase inhibitors than the reference compound ($p < 0.05$) (Table 1).

The half-inhibitory concentrations of compounds **1**, **2** and **3** demonstrated that the compounds were 213, 39 and 7 times, respectively, more potent than the complete *L. meyenii* extract for monophenolase activity (IC_{50} for **1**, **2, 3** and the extract = 0.049, 0.27, 1.49 and 10.43 μg/ml, respectively) while being 294, 72 and 10-fold, respectively, more effective than the extract for diphenolase activity (IC_{50} for **1**, **2, 3** and the extract = 0.10, 0.41, 3.09 and 29.75 μg/ml, respectively). These results indicate that the presence of **1–3** confers the anti-tyrosinase effect to the plant.

The bioassays with **1–3** showed a dose-dependent inhibitory effect with either L-tyrosine (R^2 = 0.988, 0.952 and 0.984, respectively) or L-DOPA (R^2 = 0.987, 0.954, 0.976, respectively) as substrates (Fig. 2).

Both **1** and **2** are proposed to be natural substrates of tyrosinase (Garcia-Jimenez et al., 2017) due to their resemblance, like **3**, to L-tyrosine and L-DOPA. Indeed, Garcia-Jimenez et al. (2018) described **1** and **2** as substrates of mushroom tyrosinase when added at 50 μM in presence of 4-tert-butylcatechol (TBC) and hydrogen peroxide (H_2O_2), avoiding melanin biosynthesis by diverting the pathway to different *o*-quinones. The structural similarity of the hydroxycinnamic acids to the natural ligands may lead to expect a competitive inhibition, but different results are found in literature. Regarding the inhibition on the catalysis of L-tyrosine, compound **3** was described as a competitive inhibitor of mushroom tyrosinase (Kang et al., 2004). However, as far as we know, the only kinetic study with **1** using L-tyrosine as a substrate reported the compound as a classical non-competitive inhibitor (Takahashi and Miyazawa, 2010), while no investigations regarding the type of inhibition of **2** with this substrate have been carried out. With L-DOPA as substrate, contradictory results are found in the published literature (Garcia-Jimenez et al., 2018; Gunia-Krzyżak et al., 2018). While compound **1** was a mixed-I type inhibitor according to Lim et al. (1999), Shi et al. and Hu et al. (Hu et al., 2016; Shi et al., 2005) reported it as a competitive inhibitor. On the other hand, **2** and **3** were reported as classical non-competitive inhibitors (Lee, 2002; Lin et al., 2011b). To throw light on these discrepancies, kinetic analysis for **1–3** using both substrates was performed accompanied by a docking study.

Using a Michaelis–Menten kinetic model, V_{max} and K_m values for tyrosinase were determined as 0.017 ± 0.006 ΔAbs min^{-1} and 0.5 ± 0.1 μM, respectively, with L-tyrosine as substrate, and as 0.10 ± 0.04 ΔAbs min^{-1} and 0.4 ± 0.1 μM, respectively, with L-DOPA. The results of the kinetic analysis of inhibition for each compound under the conditions employed in the current assays are summarised in Table 2. The inhibition mechanism was also supported by

Table 1
Inhibitory effects of the isolated compounds **1–3** on tyrosinase activity.

Compound	IC_{50} (μM)[a]	
	L-Tyrosine[b]	L-DOPA[c]
1	0.30 (0.20–0.44)*	0.62 (0.48–0.81)*
2	1.50 (1.04–2.16)*	2.30 (1.12–4.75)*
3	4.14 (2.84–6.03)*	8.59 (6.59–11.20)*
kojic acid	33.45 (28.91–38.70)	38.98 (31.79–47.79)

*$p < 0.05$ compared to kojic acid.
[a] IC_{50} values and 95% confidence limits (lower, upper).
[b] Value at 10 min from the start.
[c] Value at 2 min from the start.

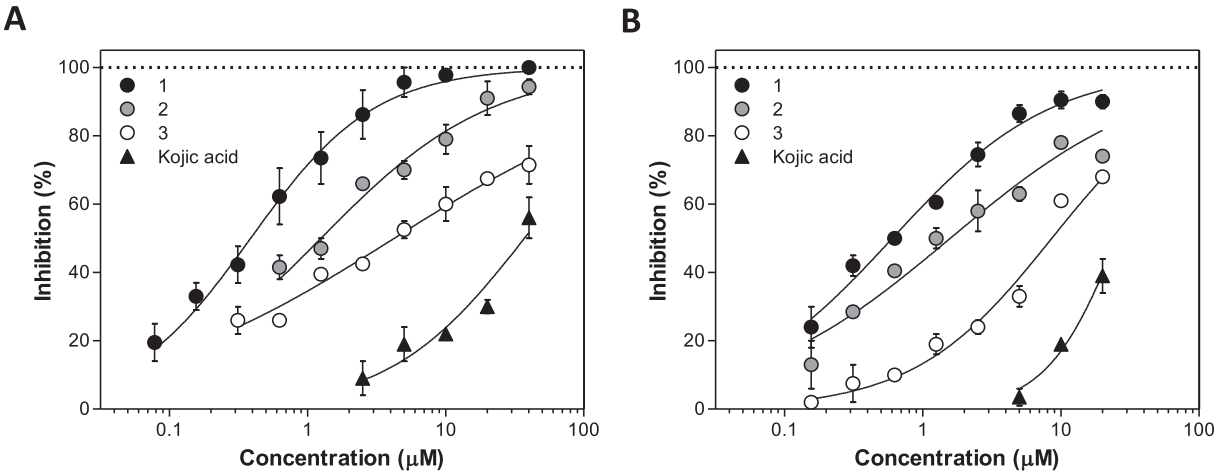

Fig. 2. Dose-dependent effect of **1**–**3**. Compounds or kojic acid were incubated with tyrosinase at 37 °C with (A) L-tyrosine or (B) L-DOPA as substrates. Data represent the mean ± SEM for two independent experiments.

Table 2
Kinetic parameters of the enzyme with L-tyrosine or L-DOPA as substrates with different concentrations of *p*-coumaric acid (**1**), caffeic acid (**2**) and rosmarinic acid (**3**).

L-Tyrosine			
Compound	K_I (μM)	αK_I (μM)	Inhibition type[a]
1	0.033	0.002	Non-competitive $\alpha < 1$ (mixed-II type)
2	2.6	2.6	Classical non-competitive $\alpha = 1$
3	7	1	Non-competitive $\alpha < 1$ (mixed-II type)
L-DOPA			
Compound	K_I (μM)	αK_I (μM)	Inhibition type[b]
1	2.2	4	Non-competitive $\alpha > 1$ (mixed-I type)
2	28	140	Non-competitive $\alpha > 1$ (mixed-I type)
3	62	62	Classical non-competitive $\alpha = 1$

[a] R^2 = 0.981, 0.830 and 0.947 for compound **1**–**3**, respectively.
[b] R^2 = 0.942, 0.973 and 0.954 for compound **1**–**3**, respectively.

the Lineweaver–Burk linear transformations and the resulting double reciprocal plot (Fig. 3). The kinetic behaviour of tyrosinase during the oxidation of L-tyrosine or L-DOPA in the presence of increasing concentrations of **2** and **3**, respectively, showed a decrease in V_{max} and an unaltered K_m (Fig. 3B and F), indicating that these are classical non-competitive inhibitors with the capacity of combining with the free enzyme and with the substrate-enzyme complex with identical affinity (Copeland, 2004). As a consequence, the equilibrium constants, K_I and αK_I, are the same (Table 2). The kinetic analysis for the other situations indicated a non-competitive inhibition of the enzyme (Table 2), with the inhibitors binding to both enzyme forms with unequal affinity (Copeland, 2004). Since inhibitors do not bind in the active site (Hsu et al., 2007; Huang et al., 2005), substrates can still bind to the enzyme-substrate complex but with a lower affinity, thus avoiding its conversion to product (Solimine et al., 2016). This kinetic type is often called mixed inhibition, with no clear differences with respect to classical non-competitive inhibitors (Solimine et al., 2016). Double-reciprocal plots of **1** (Fig. 3D) and **2** (Fig. 3E) for the oxidation of L-DOPA gave a family of straight lines which all intersected in the second quadrant. The increase of **1** and **2** concentrations resulted in a decrease of the V_{max} and in an increase of K_m. This type of inhibition is named mixed-I type inhibition. As observed in Table 2, αK_I value is greater than K_I, thus indicating a stronger affinity to the free enzyme than to the enzyme–substrate complex (Zhang et al., 2006). On the other hand, when the concentrations of **1** and **3** increased and the V_{max} and K_m for the oxidation of L-tyrosine decreased (Fig. 3A and C), a mixed-II type inhibition was observed. In this case, the value of K_I is greater than that of αK_I (Table 2), indicating that the affinity of inhibitor for the free enzyme is weaker than that for the enzyme–substrate complex (Zhang et al., 2006).

The effectiveness of compounds **1**, **2** and **3** is in good agreement with previous reports (Kang et al., 2004; Lee, 2002; Lim et al., 1999). However, to the best of our knowledge, no comparisons have been reported from the structure-activity point of view. It has been proposed that the outstanding tyrosinase inhibition of cinnamic acid derivatives relies on the presence of the double bond between the carboxyl group and the benzene ring (Robert et al., 1997), on the free carboxylic acid moiety in this simple aromatic ring which is able to chelate the cupric ions of the enzyme (Oyama et al., 2016), as well as on a 4-hydroxybenzyl group (Shi et al., 2005). While cinnamic acid showed a weak inhibitory activity on mushroom tyrosinase with an IC_{50} of 2100 μM with L-DOPA as substrate (Shi et al., 2005), compound **1** with an OH in position 4 showed stronger inhibition [IC_{50} = 0.62 μM and 500 μM as observed by Shi et al. (2005)]. An extra OH at position 3 in compound **2** decreased the activity with respect to **1**. This finding is in accordance with previous reports that the hydroxylation of the benzene ring of cinnamic acids diminished their inhibitory effect (Georgiev et al., 2013; Kermasha et al., 1993). On the other hand, the increase in the bulkiness of compound **3** due to the addition of the 3,4-dihydroxyphenyllactic acid decreased its tyrosinase inhibitor effectiveness even more compared to **2**.

The ClogP value has been previously described as a key parameter indicating lipophilicity, which is associated with better entry of the inhibitors to the active site of tyrosinase (Shao et al., 2018). Although there is no such correlation between lipophilicity and activity for compounds **1**–**3** as that observed by Shao et al. (2018) for some hydroxypyridinone derivatives, but they rather follow a non-linear behaviour as observed by Jo et al. (2017), compound **1** with the highest ClogP value, showed the greatest inhibitory effect (ClogP values were 1.57, 0.97 and 1.35 for **1**, **2** and **3**, respectively).

3.3. Molecular docking

The structural model of the *met* form of tyrosinase was first subjected to a docking simulation into a big domain, almost the whole half of the protein where the metallic site cleft and the other pockets are exposed, excluding an area which, according to the X-ray, is comprised in an intermolecular complex with a lectin-like protein. The natural substrate, L-DOPA, was also docked in addition to the subject compounds; as expected, it was found with its lowest energy cluster into the

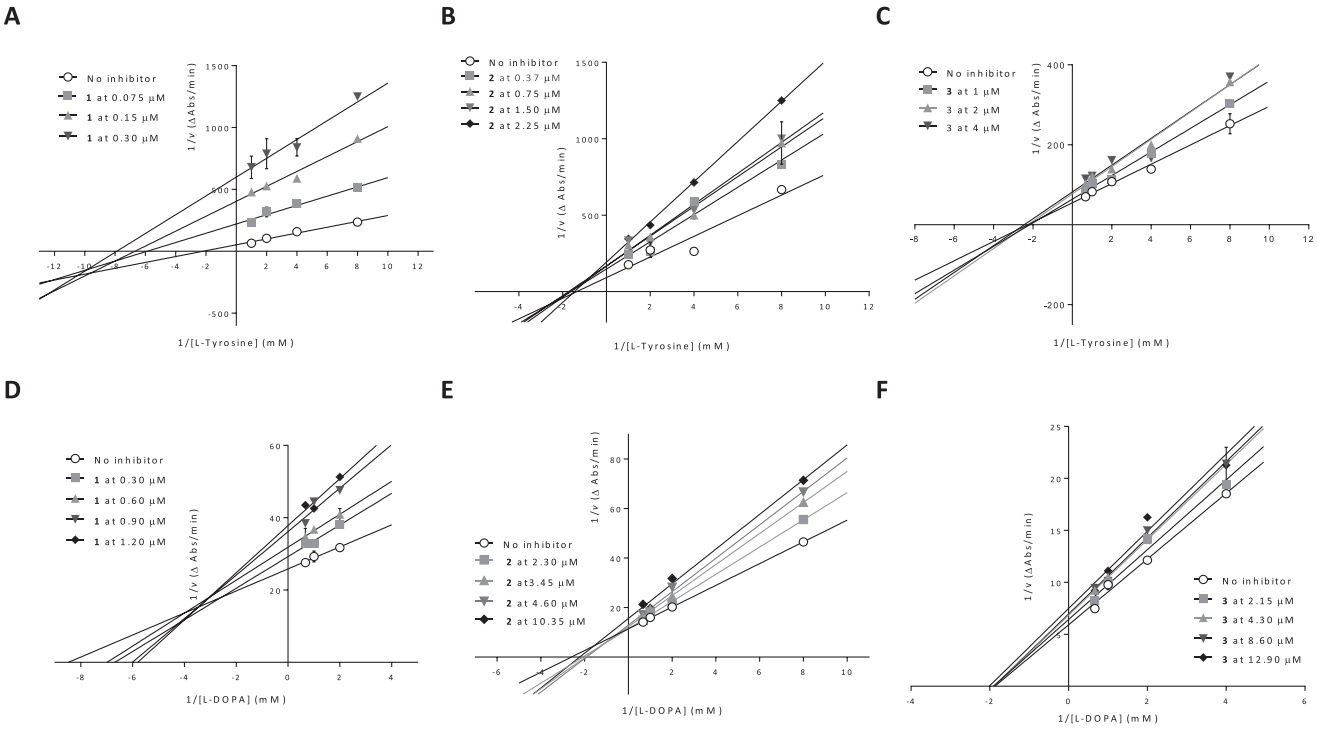

Fig. 3. Lineweaver–Burk plots in absence and presence of different concentrations of *p*-coumaric acid (**1**) (A and D), caffeic acid (**2**) (B and E) and rosmarinic acid (**3**) (C and F) for the inhibition of the oxidation of L-tyrosine (A, B and C) or L-DOPA (D, E and F). Results are expressed as mean ± SEM.

active site. This structure is shown in Fig. 4 in a putative productive pose directly interacting with the Cu—OH—Cu motif of the *met* model.

The most potent subject compounds **1** and **2** as well as the reference inhibitor kojic acid, fell within a pocket not overlapping the coordination site of the *met* protein (Fig. 4, licorice structures in magenta, green and brown, respectively), showing **1** and **2** estimated binding energies more favored than the reference inhibitor (Table 3). These results are consistent with the non-competitive type of inhibition observed for **1** and **2**, and with an increased activity with respect to the reference compound (Table 1). On the contrary, compound **3** showed a different binding mode compared to **1** and **2** (Fig. 4, licorice structure in yellow). Compound **3** also showed other binding poses of similar energy (within 0.4 kcal/mol) outside the catalytic pocket. According to the binding energy obtained (Table 3) it should be expected, at a first glance, a better inhibitory activity respect to **1** and **2**, in contrast to the experimental activity observed (Table 1). However, given than **3** showed a non-competitive behaviour and due to its interactions with different sites (and probably causing different conformational changes upon binding), the simple comparison of the estimated binding energies would not unambiguously explain the lower activity observed in comparison to **1** or **2**.

The binding mode shared by **1** and **2** was found mainly by the interactions with the residues C83, H85, G86, T87, M317, N320 and T324 (details depicted in Fig. 5). It is interesting to note that, even though the coordination site is not occluded (Fig. 5A), the interaction involves the backbone atoms of the C83 and of the Cu ligand H85, which are tightly bound through both, the backbone and a covalent thioether bond, thus forming a sort of clamp in this flexible loop. Besides, the way in which these interactions could affect the mobility of the coordination sphere in the catalytic transition state, is outside the scope of the (static) docking approach. However, this binding mode strongly suggest a plausible non-competitive inhibition. It could also suggest subtle differences between **1**, **2** and kojic acid with respect to **3**, which needs to be explored in future long term molecular dynamic studies.

Even though the extensions of the quantum and classical part are not the same regarding the *oxy* and *met* models and since the charged models are not directly comparable between them, and consequently the estimations of the binding energies, it is still possible to note a

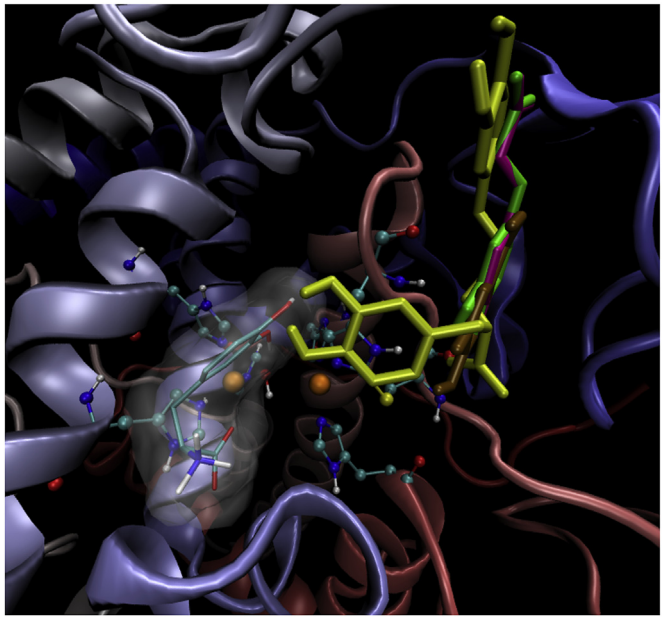

Fig. 4. *Met* model of *Agaricus bisporum* tyrosinase with the superimposition of the lowest energy poses obtained for L-DOPA (licorice, surrounded by a white translucent molecular surface), compounds **1** (licorice in magenta), **2** (green), **3** (yellow) and kojic acid (brown). The docking free energy of binding for L-DOPA was −5.44 kcal/mol. The copper ions in gold spheres surrounded by their closest residues in balls and sticks, the cartoon representation of the backbone colored according to the sequence (residues 2 to 392 from red to blue). (For interpretation of the references to colour in this figure legend, the reader is referred to the Web version of this article.)

Table 3
Estimated free energies of binding from the docking analysis of the *met* and *oxy* tyrosinase.

Compound	*Met* tyrosinase		*Oxy tyrosinase*	
	ΔG_b^0 (kcal/mol)	in the coordination site?	ΔG_b^0 (kcal/mol)	in the coordination site?
kojic acid	−4.35	no	−4.64	no
1	−4.91	no	−5.39	no
2	−5.40	no	−5.48	no
3	−8.77	no	−7.84	no

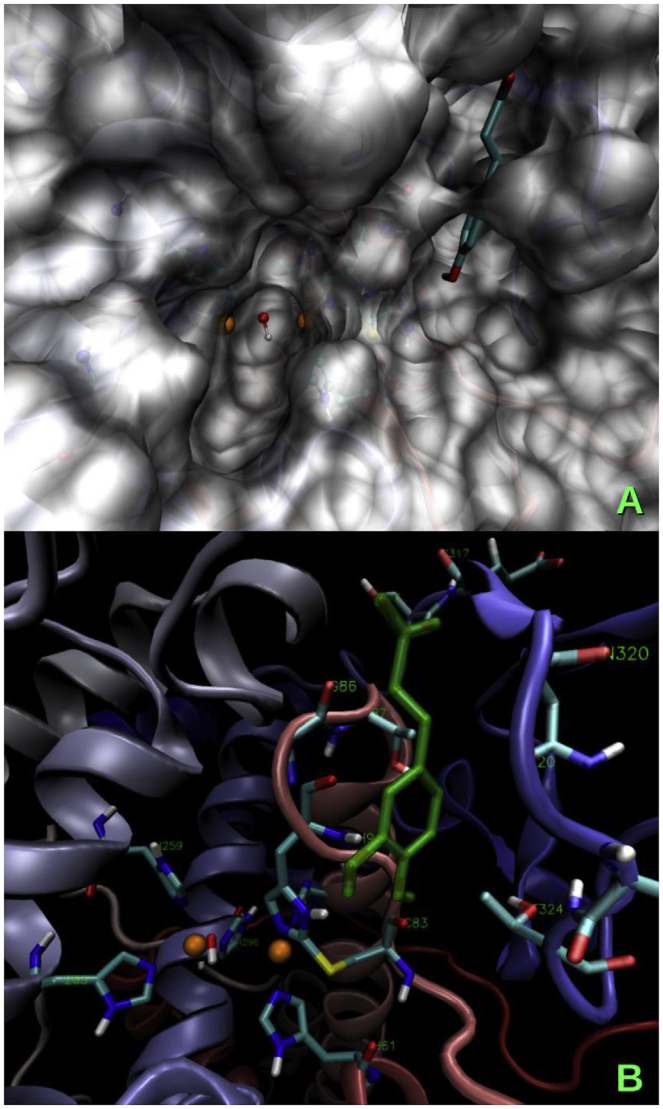

Fig. 5. A) Molecular surface of the *met* model of tyrosinase: ions as golden spheres, compound **1** in licorice. The pocket occupied by the inhibitor did not occlude the entrance of the catalytic site. B) Main contacts of the lowest energy pose of compound **2**. (For interpretation of the references to colour in this figure legend, the reader is referred to the Web version of this article.)

common feature, *i. e.* the binding outside the coordination site for the three subject compounds with the *oxy* tyrosinase. This region found as the primary binding site for **1, 2** and kojic acid into the *met* form is roughly the same for kojic acid in the *oxy* form, but it is a secondary binding site for **1** and **2**, with affinities 0.2–1.0 kcal/mol less favored than for the main binding site. This main site is even farther from the coordination site than for the case of the *met* form of tyrosinase. A comparison of the poses similar to those shown in Fig. 4, is available for the *oxy* form of the enzyme in Fig. S2 (Supplementary material).

3.4. Enrichment of L. meyenii extract

Considering that the compounds isolated from *L. meyenii* as anti-tyrosinase agents were all hydroxycinnamic acid derivatives and to further improve the activity of the extract, a phenolic fractionation step was carried out, using the method described by Chirinos et al. (2008) with some modifications. As shown in Fig. 6A, the total phenolic content increased 2.53 times with respect to that of the complete extract ($p < 0.01$). Additionally, the enriched-phenolic fraction was characterised by HPLC-DAD to allow the quantification of compounds **1–3**. A representative chromatogram obtained at 320 nm is shown in Fig. 6B. The amount of each compound per 100 g of phenolic fraction was 116 mg for **1**, 210 mg for **2** and 1109 mg for **3**. This means that the quantity of each compound was 3.4 times higher than the quantity observed in 100 g of the whole ethanol extract.

Subsequently, the inhibitory activity of the phenolic fraction was compared with the activity of the ethanol extract. As shown in Table 4, the enrichment method led to a significant 2.9-fold increase in both monophenolase and diphenolase anti-tyrosinase activity.

These results match well those described by Lee et al., who found an important correlation between the total phenol content and anti-tyrosinase activity of four species of Lamiaceae, three of them in the genus *Lavandula, L. stoechas* subsp. *pedunculata*, *L. latifolia*, and *L. allardii* 'Rly' and *Origanum majorana* (Lee et al., 2011).

The Lamiaceae family has been considered as a source of compounds that are appreciated for health care due to their high content of phenolic compounds (Trivellini et al., 2016). Within this family, *L. meyenii* stands out as having among the highest content of total phenolic compounds among 27 species with traditional uses in the Andean region studied (Chirinos et al., 2013).

3.5. Cytotoxicity on peripheral blood mononuclear cells (PBMC)

The most important thing about a tyrosinase inhibitor is that it must be safe, especially when used in food products. To determine whether compounds **1–3**, the phenolic fraction or the whole extract were toxic on normal human cells, PBMC were obtained. An MTT assay showed that compounds **1–3** were not toxic to PBMC at concentrations of up to 500 μM, a value much higher than the IC_{50} required for the anti-tyrosinase effect of these metabolites (Table 1). For the whole extract, the IC_{50} was 80.65 μg/ml (95% confidence limits (lower and upper) = 61.2 to 106.3) and no cytotoxic effect was found for the phenolic fraction at concentrations of up to 100 μg/ml. In addition to the absence of cytotoxicity described here, several health benefits have been ascribed to compounds **1–3** (Liu, 2004; Trivellini et al., 2016), with biological activities including antioxidant, anticancer, antiatherogenic, prevention of metabolic disorders, antimicrobial and anti-inflammatory effects (Lee et al., 2011; Pei et al., 2016; Trivellini et al., 2016).

4. Conclusions

This is the first report about the compounds causing the tyrosinase inhibitory effect of *L. meyenii* as well as the methodology to enrich the extract in the non-toxic anti-tyrosinase compounds **1–3** which resulted in an increased activity. The improved tyrosinase inhibition translates to a greater potential as an anti-browning food additive. This study thus validates *L meyenii* as a rich source of products with potent tyrosinase inhibitory activity. On the other hand, a joint study about the kinetic behaviour of **1–3** with both L-tyrosinase and L-DOPA as substrates was performed together with a novel docking analysis confirming in part, the results obtained. A non-competitive mechanism is proposed for the subject compounds, although with different nuances in the case of the largest and most flexible compound **3**. In addition, it was determined

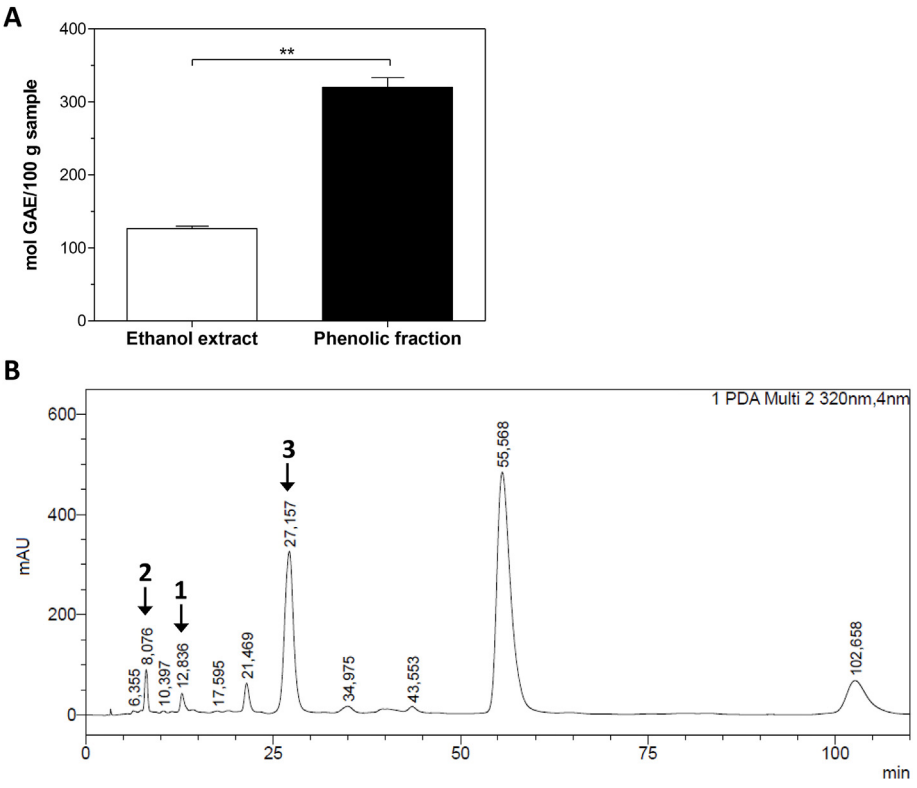

Fig. 6. A) Total phenolic content expressed in mol of gallic acid equivalents (GAE) per 100 g of sample. Data are expressed as the mean values ± SEM of two independent experiments, $^{**}p < 0.01$. B) Analytical HPLC profile of the phenolic fraction of *L. meyenii* at 10 mg/ml in methanol. The arrows indicate compounds **1**, **2** and **3**. The mobile phase was methanol/water/perchloric acid 40:60:0.05 and UV detection at 320 nm.

Table 4
Inhibitory effects of the complete extract and of the phenolic fraction on tyrosinase activity.

Products	IC_{50} (μg/ml)[a]	
	L-Tyrosine[b]	L-DOPA[c]
Ethanol extract	10.43 (4.45–24.42)	29.75 (25.53–34.67)
Phenolic fraction	3.59 (2.09–6.15)*	10.40 (5.72–18.91)*

$^{*}p < 0.05$ compared to ethanol extract.
[a] IC_{50} values and 95% confidence limits (lower, upper).
[b] Value at 10 min from the start.
[c] Value at 2 min from the start.

that compounds **1–3** were more effective at inhibiting tyrosinase than the well-known inhibitor, kojic acid.

Conflicts of interest

The authors declare that they have no conflicts of interest.

Acknowledgements

We thank Joss Heywood for revising the English language. M.B. Joray, S.M. Palacios, M. A. Vera and M.C. Carpinella are staff members of the National Research Council of Argentina (CONICET). This research project was conducted with support from the Catholic University of Cordoba, CONICET (PIP 11220100100236), PICT 2014-1594. MIC. MFC and PAL acknowledge receipt of a Scholarship from CONICET.

Appendix A. Supplementary data

Supplementary data to this article can be found online at https://doi.org/10.1016/j.fct.2019.01.019.

Transparency document

Transparency document related to this article can be found online at https://doi.org/10.1016/j.fct.2019.01.019.

References

Ainsworth, E.A., Gillespie, K.M., 2007. Estimation of total phenolic content and other oxidation substrates in plant tissues using Folin-Ciocalteu reagent. Nat. Protoc. 2, 875–877.
An, S.M., Lee, S.I., Choi, S.W., Moon, S.W., Boo, Y.C., 2008. p-Coumaric acid, a constituent of Sasa quelpaertensis Nakai, inhibits cellular melanogenesis stimulated by α-melanocyte stimulating hormone. Br. J. Dermatol. 159, 292–299.
Atanasov, A.G., Waltenberger, B., Pferschy-Wenzig, E.M., Linder, T., Wawrosch, C., Uhrin, P., Temml, V., Wang, L., Schwaiger, S., Heiss, E.H., Rollinger, J.M., Schuster, D., Breuss, J.M., Bochkov, V., Mihovilovic, M.D., Kopp, B., Bauer, R., Dirsch, V.M., Stuppner, H., 2015. Discovery and resupply of pharmacologically active plant-derived natural products: a review. Biotechnol. Adv. 33, 1582–1614.
Bart, H.-J., Pilz, S., 2011. Industrial Scale Natural Products Extraction. John Wiley & Sons.
Bayly, C.I., Cieplak, P., Cornell, W., Kollman, P.A., 1993. A well-behaved electrostatic potential based method using charge restraints for deriving atomic charges: the RESP model. J. Phys. Chem. 97, 10269–10280.
Besler, B.H., Merz Jr., K.M., Kollman, P.A., 1990. Atomic charges derived from semi-empirical methods. J. Comput. Chem. 11, 431–439.
Bruno, M., Savona, G., Piozzi, F., Maria, C., Rodriguez, B., Marlier, M., 1991. Abietane diterpenoids from Lepechinia meyeni and Lepechinia hastata. Phytochemistry 30, 2339–2343.
Burdock, G.A., Soni, M.G., Carabin, I.G., 2001. Evaluation of health aspects of kojic acid in food. Regul. Toxicol. Pharmacol. 33, 80–101.
Carpinella, M.C., Rai, M., 2009. Novel Therapeutic Agents from Plants. Science publishers.
Castillo, P., Lock, O., 2005. Compuestos con actividad antioxidante en la especie Lepechinia meyenii (Walp). Rev. Soc. Quim. Peru 71, 227.
Cespedes, C.L., Molina, S.C., Muñoz, E., Lamilla, C., Alarcon, J., Palacios, S.M., Carpinella, M.C., Avila, J.G., 2013. The insecticidal, molting disruption and insect growth inhibitory activity of extracts from Condalia microphylla Cav. (Rhamnaceae). Ind. Crop. Prod. 42, 78–86.
Chiari, M.E., Joray, M.B., Ruiz, G., Palacios, S.M., Carpinella, M.C., 2010. Tyrosinase inhibitory activity of native plants from central Argentina: isolation of an active principle from Lithrea molleoides. Food Chem. 120, 10–14.
Chiari, M.E., Vera, D.M.A., Palacios, S.M., Carpinella, M.C., 2011. Tyrosinase inhibitory activity of a 6-isoprenoid-substituted flavanone isolated from Dalea elegans. Bioorg. Med. Chem. 19, 3474–3482.
Chirinos, R., Campos, D., Costa, N., Arbizu, C., Pedreschi, R., Larondelle, Y., 2008. Phenolic profiles of andean mashua (Tropaeolum tuberosum Ruíz & Pavón) tubers:

identification by HPLC-DAD and evaluation of their antioxidant activity. Food Chem. 106, 1285–1298.
Chirinos, R., Pedreschi, R., Rogez, H., Larondelle, Y., Campos, D., 2013. Phenolic compound contents and antioxidant activity in plants with nutritional and/or medicinal properties from the Peruvian Andean region. Ind. Crop. Prod. 47, 145–152.
Clemente, F.R., Vreven, T., Frisch, M.J., 2010. Getting the most out of ONIOM: guidelines and pitfalls. Quant. Biochem. 61–83.
Coates, C.J., Nairn, J., 2013. Hemocyanin-derived phenoloxidase activity: a contributing factor to hyperpigmentation in Nephrops norvegicus. Food Chem. 140, 361–369.
Copeland, R.A., 2004. Enzymes: a Practical Introduction to Structure, Mechanism, and Data Analysis. John Wiley & Sons.
de la Cruz, M.G., Malpartida, S.B., Santiago, H.B., Jullian, V., Bourdy, G., 2014. Hot and cold: medicinal plant uses in Quechua speaking communities in the high Andes (Callejon de Huaylas, Ancash, Peru). J. Ethnopharmacol. 155, 1093–1117.
Friedman, M., 1996. Food browning and its Prevention: an overview. J. Agric. Food Chem. 44, 631–653.
Garcia-Jimenez, A., Munoz-Munoz, J.L., Garcia-Molina, F., Teruel-Puche, J.A., Garcia-Canovas, F., 2017. Spectrophotometric characterization of the action of tyrosinase on p-coumaric and caffeic acids: characteristics of o-caffeoquinone. J. Agric. Food Chem. 65, 3378–3386.
Garcia-Jimenez, A., García-Molina, F., Teruel-Puche, J.A., Saura-Sanmartin, A., Garcia-Ruiz, P.A., Ortiz-Lopez, A., Rodríguez-López, J.N., Garcia-Canovas, F., Munoz-Munoz, J., 2018. Catalysis and inhibition of tyrosinase in the presence of cinnamic acid and some of its derivatives. Int. J. Biol. Macromol. 119, 548–554.
Georgiev, L., Chochkova, M., Totseva, I., Seizova, K., Marinova, E., Ivanova, G., Ninova, M., Najdenski, H., Milkova, T., 2013. Anti-tyrosinase, antioxidant and antimicrobial activities of hydroxycinnamoylamides. Med. Chem. Res. 22, 4173–4182.
Gonzalez, M.L., Vera, D.M.A., Laiolo, J., Joray, M.B., Maccioni, M., Palacios, S.M., Molina, G., Lanza, P.A., Gancedo, S., Rumjanek, V., Carpinella, M.C., 2017. Mechanism underlying the reversal of drug resistance in P-Glycoprotein-Expressing leukemia cells by pinoresinol and the study of a derivative. Front. Pharmacol. 8, 205.
Gonzalez, M.L., Joray, M.B., Laiolo, J., Crespo, M.I., Palacios, S.M., Ruiz, G.M., Carpinella, M.C., 2018. Cytotoxic activity of extracts from plants of central Argentina on sensitive and multidrug-resistant leukemia cells: isolation of an active principle from gaillardia megapotamica. Evid. Based Complement Altern. Med.: eCAM 2018, 9185935.
Gunia-Krzyżak, A., Słoczyńska, K., Popiół, J., Koczurkiewicz, P., Marona, H., Pękala, E., 2018. Cinnamic acid derivatives in cosmetics-current use and future prospects. Int. J. Cosmet. Sci. https://doi.org/10.1111/ics.12471.
Hammond, G.B., Fernandez, I.D., Villegas, L.F., Vaisberg, A.J., 1998. A survey of traditional medicinal plants from the Callejon de Huaylas, Department of Ancash, Peru. J. Ethnopharmacol. 61, 17–30.
He, Q., Luo, Y., Chen, P., 2008. Elucidation of the mechanism of enzymatic browning inhibition by sodium chlorite. Food Chem. 110, 847–851.
Hsu, C.-K., Chang, C.-T., Lu, H.-Y., Chung, Y.-C., 2007. Inhibitory effects of the water extracts of Lavendula sp. on mushroom tyrosinase activity. Food Chem. 105, 1099–1105.
Hu, Y.-H., Chen, Q.-X., Cui, Y., Gao, H.-J., Xu, L., Yu, X.-Y., Wang, Y., Yan, C.-L., Wang, Q., 2016. 4-Hydroxy cinnamic acid as mushroom preservation: anti-tyrosinase activity kinetics and application. Int. J. Biol. Macromol. 86, 489–495.
Huang, K.-F., Chen, Y.-W., Chang, C.-T., Chou, S.-T., 2005. Studies on the inhibitory effect of Graptopetalum paraguayense E. Walther extracts on mushroom tyrosinase. Food Chem. 89, 583–587.
Humphrey, W., Dalke, A., Schulten, K., 1996. VMD: visual molecular dynamics. J. Mol. Graph. 14, 33–38.
Ismaya, W.T., Rozeboom, H.J., Weijn, A., Mes, J.J., Fusetti, F., Wichers, H.J., Dijkstra, B.W., 2011. Crystal structure of Agaricus bisporus mushroom tyrosinase: identity of the tetramer subunits and interaction with tropolone. Biochemistry (Mosc.) 50, 5477–5486.
Jo, H., Choi, M., Sim, J., Viji, M., Li, S., Lee, Y.H., Kim, Y., Seo, S.Y., Zhou, Y., Lee, K., Kim, W.J., Hong, J.T., Lee, H., Jung, J.K., 2017. Synthesis and biological evaluation of caffeic acid derivatives as potent inhibitors of alpha-MSH-stimulated melanogenesis. Bioorg. Med. Chem. Lett 27, 3374–3377.
Joray, M.B., Gonzalez, M.L., Palacios, S.M., Carpinella, M.C., 2011. Antibacterial activity of the plant-derived compounds 23-methyl-6-O-desmethylauricepyrone and (Z,Z)-5-(trideca-4,7-dienyl)resorcinol and their synergy with antibiotics against methicillin-susceptible and -resistant Staphylococcus aureus. J. Agric. Food Chem. 59, 11534–11542.
Joray, M.B., Trucco, L.D., Gonzalez, M.L., Napal, G.N., Palacios, S.M., Bocco, J.L., Carpinella, M.C., 2015. Antibacterial and cytotoxic activity of compounds isolated from flourensia oolepis. Evid. Based Complement Altern. Med.: eCAM 2015, 912484.
Joray, M.B., Villafanez, F., Gonzalez, M.L., Crespo, M.I., Laiolo, J., Palacios, S.M., Bocco, J.L., Soria, G., Carpinella, M.C., 2017. P53 tumor suppressor is required for efficient execution of the death program following treatment with a cytotoxic limonoid obtained from Melia azedarach. Food Chem. Toxicol.: Int. J. Publ. Br. Ind. Biol. Res. Assoc. 109, 888–897.
Jukanti, A., 2017. Polyphenol Oxidase(s): Importance in Food Industry, Polyphenol Oxidases (PPOs) in Plants. Springer, Singapore, pp. 93–106.
Kang, H.S., Kim, H.R., Byun, D.S., Park, H.J., Choi, J.S., 2004. Rosmarinic acid as a tyrosinase inhibitors from Salvia miltiorrhiza. Nat. Prod. Sci. 10, 80–84.
Kermasha, S., Goetghebeur, M., Monfette, A., Metche, M., Rovel, B., 1993. Inhibitory effects of cysteine and aromatic acids on tyrosinase activity. Phytochemistry 34, 349–353.
Kim, Y.J., Uyama, H., 2005. Tyrosinase inhibitors from natural and synthetic sources: structure, inhibition mechanism and perspective for the future. Cell. Mol. Life Sci.: CMLS 62, 1707–1723.
Larik, F.A., Saeed, A., Channar, P.A., Muqadar, U., Abbas, Q., Hassan, M., Seo, S.Y., Bolte, M., 2017. Design, synthesis, kinetic mechanism and molecular docking studies of novel 1-pentanoyl-3-arylthioureas as inhibitors of mushroom tyrosinase and free radical scavengers. Eur. J. Med. Chem. 141, 273–281.
Lee, H.-S., 2002. Tyrosinase inhibitors of Pulsatilla cernua root-derived materials. J. Agric. Food Chem. 50, 1400–1403.
Lee, C.-J., Chen, L.-G., Chang, T.-L., Ke, W.-M., Lo, Y.-F., Wang, C.-C., 2011. The correlation between skin-care effects and phytochemical contents in Lamiaceae plants. Food Chem. 124, 833–841.
Lee, H.-S., Shin, K.-H., Ryu, G.-S., Chi, G.-Y., Cho, I.-S., Kim, H.-Y., 2012. Synthesis of small molecule-peptide conjugates as potential whitening agents. Bull. Korean Chem. Soc. 33, 3004–3008.
Lee, S.Y., Baek, N., Nam, T.G., 2016. Natural, semisynthetic and synthetic tyrosinase inhibitors. J. Enzym. Inhib. Med. Chem. 31, 1–13.
Li, A., Xuan, H., Sun, A., Liu, R., Cui, J., 2016. Preparative separation of polyphenols from water-soluble fraction of Chinese propolis using macroporous absorptive resin coupled with preparative high performance liquid chromatography. J. Chromatogr. B Anal. Technol. Biomed. Life Sci. 1012–1013, 42–49.
Lim, J.-Y., Ishiguro, K., Kubo, I., 1999. Tyrosinase inhibitory p-coumaric acid from ginseng leaves. Phytother. Res. 13, 371–375.
Lin, L., Cui, C., Wen, L., Yang, B., Luo, W., Zhao, M., 2011a. Assessment of in vitro antioxidant capacity of stem and leaf extracts of Rabdosia serra (MAXIM.) HARA and identification of the major compound. Food Chem. 126, 54–59.
Lin, L., Dong, Y., Zhao, H., Wen, L., Yang, B., Zhao, M., 2011b. Comparative evaluation of rosmarinic acid, methyl rosmarinate and pedalitin isolated from Rabdosia serra (MAXIM.) HARA as inhibitors of tyrosinase and α-glucosidase. Food Chem. 129, 884–889.
Liu, R.H., 2004. Potential synergy of phytochemicals in cancer prevention: mechanism of action. J. Nutr. 134, 3479S–3485S.
Maisuthisakul, P., Gordon, M.H., 2009. Antioxidant and tyrosinase inhibitory activity of mango seed kernel by product. Food Chem. 117, 332–341.
Morris, G.M., Goodsell, D.S., Halliday, R.S., Huey, R., Hart, W.E., Belew, R.K., Olson, A.J., 1998. Automated docking using a Lamarckian genetic algorithm and an empirical binding free energy function. J. Comput. Chem. 19, 1639–1662.
Morris, G.M., Huey, R., Lindstrom, W., Sanner, M.F., Belew, R.K., Goodsell, D.S., Ol-son, A.J., 2009. AutoDock 4 and AutoDockTools4: automated docking with selective receptor flexibility. J. Comput. Chem. 16, 2785–2791.
Oyama, T., Takahashi, S., Yoshimori, A., Yamamoto, T., Sato, A., Kamiya, T., Abe, H., Abe, T., Tanuma, S.I., 2016. Discovery of a new type of scaffold for the creation of novel tyrosinase inhibitors. Bioorg. Med. Chem. 24, 4509–4515.
Palacios, S.M., del Corral, S., Carpinella, M.C., Ruiz, G., 2010. Screening for natural inhibitors of germination and seedling growth in native plants from Central Argentina. Ind. Crop. Prod. 32, 674–677.
Pei, K., Ou, J., Huang, J., Ou, S., 2016. p-Coumaric acid and its conjugates: dietary sources, pharmacokinetic properties and biological activities. J. Sci. Food Agric. 96, 2952–2962.
Rai, M., Carpinella, M.C., 2006. Naturally Occurring Bioactive Compounds. Elsevier.
Rappé, A.K., Casewit, C.J., Colwell, K., Goddard III, W.A., Skiff, W., 1992. UFF, a full periodic table force field for molecular mechanics and molecular dynamics simulations. J. Am. Chem. Soc. 114, 10024–10035.
Robert, C., Rouch, C., Cadet, F., 1997. Inhibition of palmito (Acanthophoenix rubra) polyphenol oxidase by carboxylic acids. Food Chem. 59, 355–360.
Rojas, R., Bustamante, B., Bauer, J., Fernandez, I., Alban, J., Lock, O., 2003. Antimicrobial activity of selected Peruvian medicinal plants. J. Ethnopharmacol. 88, 199–204.
Rouet-Mayer, M.-A., Ralambosoa, J., Philippon, J., 1990. Roles of o-quinones and their polymers in the enzymic browning of apples. Phytochemistry 29, 435–440.
Shao, L.-L., Wang, X.-L., Chen, K., Dong, X.-W., Kong, L.-M., Zhao, D.-Y., Hider, R.C., Zhou, T., 2018. Novel hydroxypyridinone derivatives containing an oxime ether moiety: synthesis, inhibition on mushroom tyrosinase and application in anti-browning of fresh-cut apples. Food Chem. 242, 174–181.
Shi, Y., Chen, Q.-X., Wang, Q., Song, K.-K., Qiu, L., 2005. Inhibitory effects of cinnamic acid and its derivatives on the diphenolase activity of mushroom (Agaricus bisporus) tyrosinase. Food Chem. 92, 707–712.
Solimine, J., Garo, E., Wedler, J., Rusanov, K., Fertig, O., Hamburger, M., Atanassov, I., Butterweck, V., 2016. Tyrosinase inhibitory constituents from a polyphenol enriched fraction of rose oil distillation wastewater. Fitoterapia 108, 13–19.
Takahashi, T., Miyazawa, M., 2010. Tyrosinase inhibitory activities of cinnamic acid analogues. Die Pharm. Int. J. Pharmaceut. Sci. 65, 913–918.
Trivellini, A., Lucchesini, M., Maggini, R., Mosadegh, H., Villamarin, T.S.S., Vernieri, P., Mensuali-Sodi, A., Pardossi, A., 2016. Lamiaceae phenols as multifaceted compounds: bioactivity, industrial prospects and role of “positive-stress”. Ind. Crop. Prod. 83, 241–254.
Wu, B., 2014. Tyrosinase inhibitors from terrestrial and marine resources. Curr. Top. Med. Chem. 14, 1425–1449.
Yanai, T., Tew, D.P., Handy, N.C., 2004. A new hybrid exchange–correlation functional using the Coulomb-attenuating method (CAM-B3LYP). Chem. Phys. Lett. 393, 51–57.
Zhang, J.-P., Chen, Q.-X., Song, K.-K., Xie, J.-J., 2006. Inhibitory effects of salicylic acid family compounds on the diphenolase activity of mushroom tyrosinase. Food Chem. 95, 579–584.